

# Unexpected Gas-Phase Reactivity of the CH<sub>3</sub>OH Adduct of Michler's Hydrol Blue: Proton-Shuttle Catalysis and Stepwise Radical Expulsions

Detlef Schröder,<sup>†</sup> Jana Roithová,<sup>\*,†,‡</sup> Philipp Gruene,<sup>§</sup> Helmut Schwarz,<sup>||</sup> Herbert Mayr,<sup>⊥</sup> and Konrad Koszinowski<sup>\*,⊥</sup>

*Institute of Organic Chemistry and Biochemistry, Flemingovo nám. 2, 16610 Praha 6, Czech Republic,*

*Department of Organic Chemistry, Charles University in Prague, Faculty of Science, Hlavova 8,*

*12843 Praha 2, Czech Republic, Institut für Chemie der Technischen Universität Berlin, Strasse des 17 Juni*

*135, 10623 Berlin, Germany, and Department Chemie und Biochemie der Ludwig-Maximilians-Universität*

*München, Butenandtstrasse 5-13 (Haus F), 81377 München, Germany*

Received: May 22, 2007; In Final Form: July 9, 2007

Electrospray ionization of a methanolic solution of Michler's hydrol blue, bis(4-(*N,N*-dimethylamino)phenyl)-methyl tetrafluoroborate,  $1^+BF_4^-$ , produces the formal methanol adduct [ $1^+CH_3OH$ ], which shows an unusual gas-phase chemistry. Tandem mass-spectrometry experiments and complementary theoretical studies indicate that this adduct corresponds to the methyl ether of Michler's hydrol protonated at one of the dimethylamino groups, cation  $3^+$ . Collision-induced dissociation of mass-selected  $3^+$  leads to two sequential expulsions of open-shell species, resulting in a formal loss of  $[C_2H_6O]$ , whereas no expulsion of methanol is observed. In contrast, interaction of gaseous  $3^+$  with a single molecule of a suitable base triggers an exoergic loss of methanol via proton-shuttle catalysis within the collision complex. The occurrence of this exothermic proton transfer also prevents the application of the otherwise successful kinetic method for the determination of the gas-phase proton affinity of the methyl ether of Michler's hydrol.

## Introduction

Carbenium ions and their reactions constitute a central part of organic chemistry.<sup>1</sup> While some carbenium ions are only known as transient species,<sup>2</sup> others are remarkably stable. A prototypical example of such stable carbenium ions is Michler's hydrol blue, the bis(4-(*N,N*-dimethylamino)phenyl)methyl cation  $1^+$  (Scheme 1). The solution chemistry of  $1^+$  and related compounds has been extensively studied, because of an interest in the spectral properties of these species<sup>3,4</sup> and in the context of the development of a comprehensive nucleophilicity scale.<sup>5</sup> With a  $pK_R^+$  value of +5.61,<sup>5</sup> the free cation  $1^+$  has a significant equilibrium concentration in neutral aqueous solution. Accordingly, kinetic studies have shown the nucleophilic attack of water and alcohols at the central carbon atom of  $1^+$  to proceed only slowly and reversibly, followed by fast deprotonation and formation of the corresponding alcohol or ether, respectively.<sup>6</sup>

Surprisingly, only little is known about the gas-phase reactivities of highly stabilized carbenium ions.<sup>7–11</sup> This situation appears particularly unsatisfactory given the well-known importance of solvation effects for the reactivity of polar organic compounds. The potential-energy surfaces of  $S_N2$  reactions,<sup>12–15</sup> the basicities of amines,<sup>16</sup> and the acidities of phenols<sup>17</sup> are classical examples in which solvation may obscure the systems' intrinsic properties; i.e., the reactivity does not depend only on the reactants and products, but it is largely influenced by their stabilization due to solvation. In part, this lack of experimental

studies is due to difficulties in generating such carbenium ions in classical mass spectrometers. In contrast, electrospray ionization (ESI)<sup>18,19</sup> constitutes a versatile method for the direct transfer of ions from solution to the gas phase and thus enables the investigation of their uni- and bimolecular reactivities without the complicating effects of solvation. ESI of methanolic solutions of  $1^+$  does indeed lead to the generation of high yields of  $1^+$  along with its formal methanol adduct. Surprisingly, the latter shows an unusual gas-phase reactivity which cannot be explained from the known chemistry of  $1^+$  in solution. Here, we present our initial observations as well as more extensive studies that lead to a consistent picture of the gas-phase chemistry and energetics of the system  $1^+/CH_3OH$ .

## Experimental and Theoretical Methods

Most of the experiments were performed with a VG BIO-Q mass spectrometer, which has been described previously.<sup>20</sup> Briefly, the VG BIO-Q consists of an ESI source combined with a tandem mass spectrometer of QHQ configuration (Q stands for quadrupole and H for hexapole). In the present experiments, mmolar solutions of  $1^+BF_4^-$  in CH<sub>3</sub>OH were subjected to ESI with N<sub>2</sub> as nebulizing and drying gas at a source temperature of 80 °C. The first quadrupole was used as a mass filter to scan the ion spectrum produced or to select ions of interest. These were then guided through the hexapole serving as reaction chamber followed by mass analysis of the ionic reaction products by means of the second quadrupole and subsequent detection. Reagent or collision gases were leaked into the hexapole at typical pressures of  $(2–5) \times 10^{-4}$  mbar. The lower value of this range corresponds to approximate single-collision conditions as verified by investigation of pressure dependences. For collision-induced dissociation (CID), the mass-selected ions were subjected to collisions with xenon at variable

\* To whom correspondence should be addressed.

<sup>†</sup> Institute of Organic Chemistry and Biochemistry.

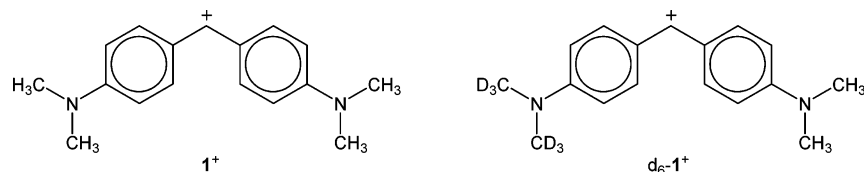
<sup>‡</sup> Charles University in Prague.

<sup>§</sup> Present address: Fritz-Haber-Institut, Faradayweg 4-5, 14195 Berlin, Germany.

<sup>||</sup> Universität Berlin.

<sup>⊥</sup> Ludwig-Maximilians-Universität München.

## SCHEME 1



collision energies  $E_{CM}$  defined as  $E_{CM} = E_{lab}m_T/(m_T + m_{ion})$ , where  $E_{lab}$  stands for the collision energy in the laboratory frame and  $m_T$  and  $m_{ion}$  are the masses of the neutral target and the ionic reactant, respectively. The investigations of thermal ion/molecule reactions described below were performed similarly at a collision energy adjusted to nominally 0 eV. In several instances, we have already demonstrated that thermal reactions can be monitored under these conditions.<sup>21–25</sup>

As pointed out previously, the VG Bio-Q does not allow a direct extraction of quantitative threshold information from CID experiments due to several limitations of the commercial instrument.<sup>20</sup> For weakly bound ions,<sup>26</sup> for example, even at  $E_{lab} = 0$  eV, a non-negligible amount of ion decay is observed. This decay is in part attributed to the kinetic energy distribution of the parent ion beam as well as the presence of collision gas not only in the hexapole but also in the focusing regions between the mass analyzers. Note that this dissociation is not caused by metastable ions because it does not occur in the absence of collision gas. The energy dependence of the product distributions in the CID spectra can be approximated by a sigmoid function suggested by Bouchoux and co-workers,<sup>27</sup> which allows extracting some semiquantitative information about the energetics of the ions examined.<sup>28</sup> For this purpose sigmoid functions of the type  $I_i(E_{CM}) = (BR_i/(1 + e^{(E_{1/2}-E_{CM})/b}))$  can be applied; for the parent ion M, the relation is  $I_M(E_{CM}) = [1 - \sum(BR_i/(1 + e^{(E_{1/2,i}-E_{CM})/b_i}))]$ . Here,  $BR_i$  stands for the branching ratio of a particular product ion ( $\sum BR_i = 1$ ),  $E_{1/2}$  is the energy at which the sigmoid function has reached half of its maximum, and  $b$  describes the rise of the sigmoid curve. Non-negligible ion decay at  $E_{lab} = 0$  eV as well as some fraction of nonfragmenting parent ions at large collision energies are accounted for by appropriate scaling and normalization procedures. The phenomenological threshold energies given below were derived from linear extrapolations of the rise of the sigmoid curves at  $E_{1/2}$  to the baseline; note, however, that the term  $E_{1/2}$  does not correspond to the intrinsic appearance energies of the fragmentation of interest, not to speak of the corresponding thermochemical thresholds at 0 K.

A few additional experiments were performed with a modified VG ZAB/HF/AMD four-sector mass spectrometer with a BEBE configuration (B stands for magnetic and E for electric sector) at the Technical University Berlin;<sup>29</sup> below, this is referred to as sector instrument (TUB). The ions of interest were generated by chemical ionization of the corresponding neutral precursor molecules indicated below and then accelerated to a kinetic energy of 8 keV and mass selected with  $B(1)/E(1)$ . The unimolecular dissociations of metastable ions (MI) or the high-energy CID spectra were recorded by scanning  $B(2)$ . To link the experiments at keV energies investigated with the Berlin sector instrument with those performed in the VG Bio-Q, compound **6** was also studied in a VG ZAB2-SEQ hybrid mass spectrometer with a BEQQ configuration, which is installed at the J. Heyrovský Institute of Physical Chemistry;<sup>30</sup> below, this is referred to as hybrid instrument (JHI). Ion generation and mass selection are almost identical with the TUB sector instrument, but the hybrid configuration allows the deceleration

of the ions to low kinetic energies, such that an energy range similar to that of the VG Bio-Q can be sampled.

The carbenium ion  $1^+$  and its labeled counterpart  $1^+-d_6$  were prepared in analogy to the method of Jutz;<sup>31</sup> for the synthesis of the latter,  $C_6H_5N(CD_3)_2$  was employed, which was made according to a literature procedure.<sup>32</sup> All other chemicals were used as purchased.

The calculations were performed using the density functional method B3LYP<sup>33</sup> in conjunction with a 6-311G\* basis set as implemented in the Gaussian 03 suite.<sup>34</sup> For all optimized structures, frequency analyses at the same level of theory were used to assign them as genuine minima or transition structures on the potential-energy surface (PES) as well as to calculate zero-point vibrational energies (ZPVEs). The relative energies ( $E_{rel}$ ) of the structures given below refer to energies at 0 K and are anchored to  $E_{rel}(8H^+) = 0.00$  eV and  $E_{rel}(9H^+) = 0.00$  eV ( $E_{0K}(8H^+) = -480.992\,323$  hartree and  $E_{0K}(9H^+) = -712.011\,850$  hartree, respectively). The minima are written in bold numbers together with the corresponding charge, and transition structures are denoted by the two numbers of the corresponding minima separated by a slash.

## Results and Discussion

As expected, electrospray ionization of a dilute solution of  $1^+BF_4^-$  in methanol gives a prominent signal with  $m/z = 253$  corresponding to  $1^+$ . In addition, the formal adduct of  $1^+$  with one solvent molecule,  $[1\cdot CH_3OH]^+$ , is formed upon ESI ( $m/z = 285$ ). Interestingly, this species shows an unexpected behavior with regard to variations of the ionization conditions in electrospray. Specifically, the electric potentials applied in those regions of the ESI source which are still close to atmospheric pressure (prior to transfer of the ions in the ultrahigh vacuum of the mass spectrometer) determine the hard- or softness of the ionization conditions via the collision energies of the incident ions with the nebulizing and drying gas nitrogen during ESI. Upon increasing the decisive potential (called “cone voltage” in the VG BioQ), not the formal adduct  $[1\cdot CH_3OH]^+$  but the parent cation  $1^+$  starts to disappear first. Such a persistence of  $[1\cdot CH_3OH]^+$  at enforced ionization conditions is in fact incompatible with the structure of a loosely bound adduct between  $1^+$  and methanol. To achieve further insight,  $[1\cdot CH_3OH]^+$  was mass-selected and subjected to CID. At a center-of-mass collision energy of  $E_{CM} \approx 2$  eV, fragmentation of  $[1\cdot CH_3OH]^+$  starts to occur with a fragment ion at  $m/z = 239$  as major product (Figure 1), which corresponds to a mass difference of  $\Delta m = -46$  and hence a neutral fragment with the composition  $[C_2H_6O]$ .

While being of rather small abundance and thus almost appearing negligible, loss of a  $CH_3$  radical ( $\Delta m = -15$ ) from  $[1\cdot CH_3OH]^+$  is observed as well and even has a significantly lower apparent threshold ( $1.7 \pm 0.4$  eV) than the formation of the major fragment at  $m/z = 239$  ( $2.7 \pm 0.2$  eV). The latter fragment largely dominates the CID spectra of  $[1\cdot CH_3OH]^+$ , however, and only at  $E_{CM} > 6$  eV do further fragmentations start to take place, such as formation of a fragment ion with  $m/z = 223$  (not shown in Figure 1). Importantly, loss of

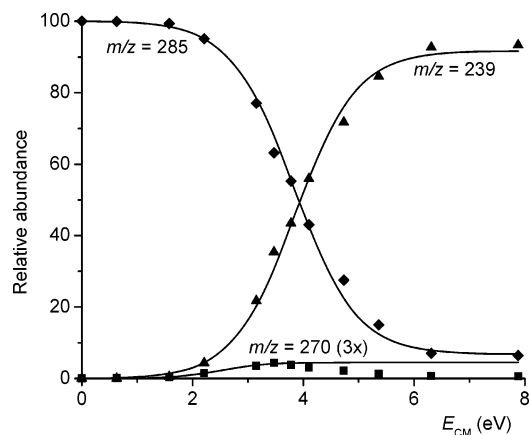


**Figure 1.** Relative abundances of the parent ion ( $m/z = 285$ , symbol  $\blacklozenge$ ) and daughter ions ( $m/z = 239$ , symbol  $\blacktriangle$ ;  $m/z = 270$ , symbol  $\blacksquare$ , multiplied by a factor of 3) as a function of collision energy (center-of-mass) upon CID of mass-selected  $[\mathbf{1}\cdot\text{CH}_3\text{OH}]^+$ . The lines represent fits of the ion abundances using a sigmoid function; see experimental details. The apparent thresholds for  $m/z = 239$  and  $m/z = 270$  are  $2.7 \pm 0.2$  and  $1.7 \pm 0.4$  eV, respectively. Note that the fit for  $m/z = 270$  fails to reproduce the experimentally measured abundance above the threshold of the competing channel to  $m/z = 239$ .

methanol ( $\Delta m = -32$ ) is not observed at all upon CID of ion  $[\mathbf{1}\cdot\text{CH}_3\text{OH}]^+$ , which again strongly suggests that the structure of  $[\mathbf{1}\cdot\text{CH}_3\text{OH}]^+$  does not correspond to a loosely bound adduct of  $\mathbf{1}^+$  and methanol.

To further probe the identity of  $[\mathbf{1}\cdot\text{CH}_3\text{OH}]^+$ , the solvent was changed from CH<sub>3</sub>OH to CD<sub>3</sub>OD. As expected, the signal corresponding to  $\mathbf{1}^+$  is not affected and remains at  $m/z = 253$ , whereas the signal at  $m/z = 285$  shifts upward by 4 mass units to  $m/z = 289$ , obviously corresponding to the formal adduct of  $\mathbf{1}^+$  with perdeuteromethanol  $[\mathbf{1}\cdot\text{CD}_3\text{OD}]^+$ . Upon CID, the labeled species  $[\mathbf{1}\cdot\text{CD}_3\text{OD}]^+$  yields an ion with  $m/z = 240$ , which thus contains only a single deuterium atom; in turn, the neutral fragment lost,  $[\text{C}_2\text{H}_3\text{D}_3\text{O}]$  ( $\Delta m = -49$ ), comprises the remaining three D atoms. In addition, we investigated the formal methanol adduct of the carbenium ion with one of the two *N,N*-dimethylamino groups fully deuterated,  $[\mathbf{1}\cdot\text{CH}_3\text{OH}-d_6]^+$  ( $m/z = 291$ ). CID yields two ionic fragments with  $m/z = 242$  and 245 (losses of  $[\text{C}_2\text{H}_3\text{D}_3\text{O}]$  and  $[\text{C}_2\text{H}_6\text{O}]$ , respectively), consistent with incorporation of one of the *N*-methyl groups in the neutral fragment lost. The expulsion of the deuterated fragment is slightly preferred, hence giving rise to an inverse kinetic isotope effect of  $\text{KIE} = 0.90 \pm 0.10$ ; we note that the latter quantity does not show a significant dependence on the collision energy.<sup>26</sup>

The results obtained so far permit some preliminary conclusions with regard to the structure of the formal adduct  $[\mathbf{1}\cdot\text{CH}_3\text{OH}]^+$ . Three options are conceivable (Scheme 2), of which the first corresponds to the oxonium ion  $\mathbf{2}^+$ . Alternatively, a sequence of de- and reprotonation reactions may lead to the ammonium ion  $\mathbf{3}^+$  or the formation of ring-protonated isomers as represented by structure  $\mathbf{4}^+$ . The labeling experiments strongly suggest that the dominant elimination of fragment  $[\text{C}_2\text{H}_6\text{O}]$  contains one methyl group originally bonded to a nitrogen atom and the methoxy group originating from the solvent (CH<sub>3</sub>OH). Thus, the methoxy group remains intact in the course of the reaction. The absence of CH<sub>3</sub>OH elimination further excludes O-protonation under ESI conditions, i.e., structure  $\mathbf{2}^+$ . Instead, the remaining proton can be located at one of the two, much more basic dimethylamino groups leading to structure  $\mathbf{3}^+$ , or formation of ring-protonated isomers ( $\mathbf{4}^+$ ) can be suggested. Although protonation at the ring is conceivable in general, thermochemical considerations very much favor the formation

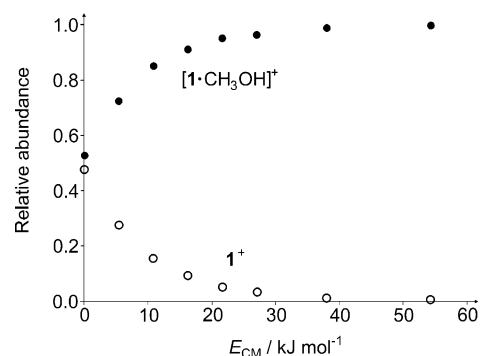


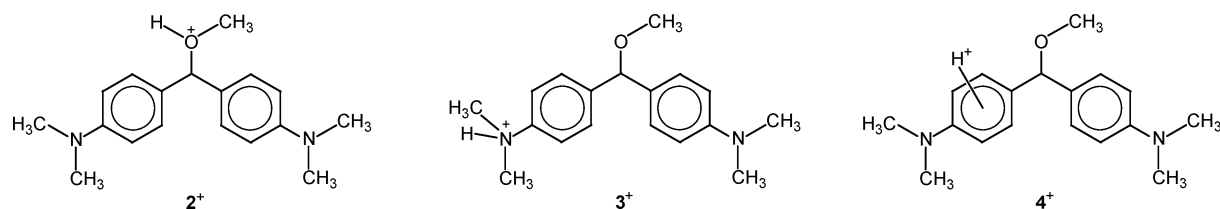
**Figure 2.** Relative abundances of the parent ion  $[\mathbf{1}\cdot\text{CH}_3\text{OH}]^+$  and the daughter ion  $\mathbf{1}^+$  in the reaction of  $[\mathbf{1}\cdot\text{CH}_3\text{OH}]^+$  with NH<sub>3</sub> as functions of the collision energy  $E_{CM}$ .

of  $\mathbf{3}^+$ , because the proton affinity of the dimethylamino group is significantly larger than that of the ring.<sup>35</sup> The ion  $[\mathbf{1}\cdot\text{CH}_3\text{OH}]^+$  is hence assigned to have structure  $\mathbf{3}^+$ .

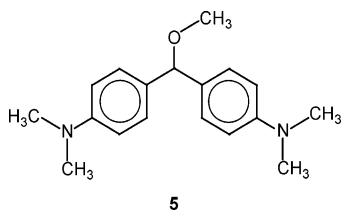
**Proton-Shuttle Catalysis.** Given that structure  $\mathbf{3}^+$  bears an sp<sup>3</sup>-hybridized central carbon atom and thus suspends the energetically favorable conjugation between the two aromatic rings, its dissociation into  $\mathbf{1}^+$  and CH<sub>3</sub>OH might well be exoergic. However, this dissociation needs to be initiated by hydrogen rearrangement, which is obviously hindered by a barrier. Prompting this reaction to occur would require a significant lowering of the barrier associated with proton transfer. This special case of catalysis might be achieved by so-called proton shuttles.<sup>36–41</sup> As the name already implies, these catalyst species can accept a proton from one site of a molecule and release it at another, spatially distant one. Obviously, this ability requires the presence of a vacant basic coordination site in the shuttle molecule.

A simple compound potentially capable of mediating proton transfer is ammonia. Exposure of mass-selected  $[\mathbf{1}\cdot\text{CH}_3\text{OH}]^+$ , that is tautomer  $\mathbf{3}^+$ , to NH<sub>3</sub> at a collision energy nominally set to zero does indeed yield free  $\mathbf{1}^+$  as ionic product. As expected for a thermal ion/molecule reaction mediated by a long-lived collision complex, the product-ion yield readily diminishes with increasing kinetic energy, thus proving the exoergic character of this process (Figure 2). Note that for an endoergic process, such as CID, the opposite behavior would be expected. If the role of NH<sub>3</sub> is in fact limited to that of a mere proton shuttle, other bases should catalyze the dissociation of  $\mathbf{3}^+$  as well. H/D exchange reactions of numerous protonated substances have been shown to proceed in the gas phase as long as the endothermicity of the proton transfer between the reactant pair is lower than 100 kJ mol<sup>-1</sup>, which is the amount of energy typically provided by the formation of proton-bound dimers.<sup>42,43</sup> A similar situation may be anticipated for the present case where a series of bases was tested to probe a possible correlation between their proton affinities (PAs) and their abilities to mediate the dissociation of  $\mathbf{3}^+$  (Table 1). As the data show, the different bases probed do not exhibit a strict correlation between their PA and their catalytic activity in terms of mediating the dissociation of gaseous  $\mathbf{3}^+$ . Apparently, the deviations observed reflect slight differences in the complexation energies as well as different steric demands of the various bases in the proton-transfer process. Specifically, the ability of NH<sub>3</sub> to induce methanol loss can be ascribed to the small size of this molecule, which should allow a particularly facile proton transport. In contrast, 1,2-dimethoxyethane and methyl vinyl ether do not mediate the loss of neutral methanol although they have higher PAs than NH<sub>3</sub>. This deviating behavior can be attributed to the specific properties of these two oxygen bases. 1,2-Dimethoxy-

## SCHEME 2



## SCHEME 3



## SCHEME 4

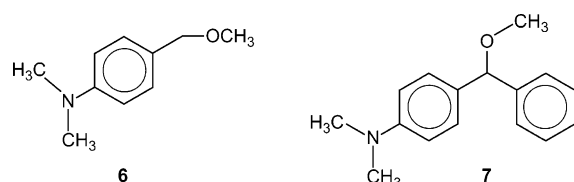


**TABLE 1: Dissociation of Mass-Selected  $3^+$  in Thermal Ion/Molecule Reactions with Various Neutral Reference Bases **B** as a Function of  $PA(\mathbf{B})$ <sup>47</sup>**

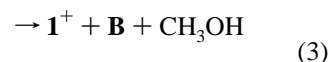
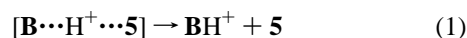
external base	$PA(\mathbf{B})$ ( $\text{kJ mol}^{-1}$ )	dissociation of $3^+$	proton transfer
methanol	754.3	—	—
isobutene	802.1	—	—
diethyl ether	828.4	—	—
cyclohexanone	841.0	—	—
ammonia	853.6	+	—
1,2-dimethoxyethane	858.0	—	—
methyl vinyl ether	859.2	—	—
<i>N,N</i> -dimethylformamide	887.5	+	—
methylamine	899.0	+	—
pyridine	930.0	+	—
triethylamine	981.8	+	+

ethane bears two basic sites whose combined interaction gives rise to the large PA of this ether. Upon approach of this reagent to a sterically demanding species such as  $3^+$ , however, it is likely that only one of the two oxygen atoms can effectively interact with the proton at the dimethylamino substituent in  $3^+$ . Hence, the effective PA in proton-transfer catalysis may be closer to that of a single ether linkage, i.e.,  $PA(\text{C}_2\text{H}_5\text{OC}_2\text{H}_5) = 828.4 \text{ kJ mol}^{-1}$  (Table 1).

In the case of methyl vinyl ether, a possible explanation for the absence of proton-transfer catalysis is associated with the fact that protonation does not take place at the heteroatom, but rather the double bond of the vinyl group is attacked. Thus, proton transfer from the ammonium group in  $3^+$  to  $\text{CH}_3\text{OCH}=\text{CH}_2$  is likely to be associated with a barrier, because rehybridization of the C–C bond is necessary and due to the charge delocalization also rehybridization of the C–O bond is required.

For a more detailed understanding of the proton-shuttle catalysis, the knowledge of the PA of the corresponding neutral ether **5** is desirable. We attempted to solve this problem by application of the kinetic method developed by Cooks, which has been successfully used in numerous similar cases.<sup>44</sup> Addition of a base **B** of appropriate strength to a solution of  $1^+$  in  $\text{CH}_3\text{-OH}$  and ESI of this mixture yields proton-bound dimers which

formally correspond to  $[\mathbf{B}\cdots\text{H}^+\cdots\mathbf{5}]$ . CID of such a complex should hence produce the ionic products  $\mathbf{BH}^+$ , reaction 1, and  $3^+$ , reaction 2. According to the kinetic method, the ratio of the abundances of these fragments can be correlated with their relative thermochemical stabilities, i.e.,  $\Delta PA$ .<sup>45</sup> Therefore, we applied *N*-methylpyrrolidine ( $PA = 966 \text{ kJ mol}^{-1}$ ), diisopropylamine ( $PA = 972 \text{ kJ mol}^{-1}$ ), and triethylamine ( $PA = 982 \text{ kJ mol}^{-1}$ ) as reference bases **B**, which all yield reasonably abundant aggregates of the type  $[\mathbf{B}\cdots\text{H}^+\cdots\mathbf{5}]$ .<sup>46,47</sup> In the CID experiments, however, not only the two expected fragmentation products  $\mathbf{BH}^+$  and  $3^+$  according to reactions 1 and 2 but also bare  $1^+$  is observed as a fragment in significant amounts.



The formation of  $1^+$  is indeed not too surprising because the results presented above have already shown that the presence of a base **B** can induce the dissociation of  $3^+$  into  $1^+$  and methanol (reaction 3). The actual amount of  $3^+$  being observed as a result of the CID process does therefore not only depend on the difference of the proton affinities of the reference base **B** and the neutral ether **5** but also on the efficiency of the reference base to act as a catalyst for the proton transfer. In the present case, this competition leads to an inapplicability of the kinetic method, in that no clear correlation between the ratio of the ionic products due to reactions 1 and 2 and  $PA(\mathbf{B})$  was obtained. This failure is by no means due to the kinetic method itself but inherently connected with the particular nature of the ion under study, specifically, with the fact that the reference bases can also act as proton-shuttle catalysts. Nevertheless, the data obtained suggest a  $PA(\mathbf{5})$  between 955 and 965  $\text{kJ/mol}$  as a crude estimate, which is similar to the known value for the structurally related compound 4-(*N,N*-dimethylamino)toluene,  $PA((\text{CH}_3)_2\text{NC}_6\text{H}_4\text{CH}_3) = 950 \text{ kJ/mol}$ .<sup>47</sup>

**Mechanism of  $[\text{C}_2\text{H}_6\text{O}]$  Loss.** Having established the exothermicity of the kinetically hindered loss of methanol from  $3^+$ , we can now address the kinetically favored loss of  $[\text{C}_2\text{H}_6\text{O}]$  observed upon CID in more detail. As discussed above, the labeling experiments unequivocally show that the expelled  $[\text{C}_2\text{H}_6\text{O}]$  fragment comprises the intact  $\text{OCH}_3$  group and one of the *N*-methyl groups of  $3^+$ . Hydrogen scrambling involving these groups does not take place. Combination of these two fragments would yield dimethyl ether as a stable and thus thermochemically favored species. However, formation of dimethyl ether is difficult to rationalize because such a process would involve the migration of one methyl group from the protonated dimethylamino group across the arene spacer to the methoxy group in the center of the molecule. As the migration of a proton across the skeleton of  $3^+$  does not occur under the experimental conditions, it seems improbable that the migration of a methyl group would be more facile under identical

**TABLE 2: Mass Differences ( $\Delta m$ ) and Relative Fragment Abundances<sup>a</sup> Observed in the Fragmentation of Mass-Selected 6H<sup>+</sup> under Different Conditions**

no.	instrument	ionization <sup>b</sup>	expt <sup>c</sup>	-15	-31	-32	-46
1	multipole (TUB)	ESI (CH <sub>3</sub> OH)	CID (8 eV)	100		2	10
2		ESI (CH <sub>3</sub> OH)	CID (15 eV)	100	2	4	55
3		ESI (CH <sub>3</sub> OH)	CID (30 eV)	40	8	4	100
4	sector (TUB)	CI (H <sub>2</sub> O)	MI	10	5	100	2
5		CI (C <sub>4</sub> H <sub>10</sub> )	MI	15	5	100	2
6		CI (NH <sub>3</sub> )	MI	50	5	100	3
7		CI (H <sub>2</sub> O)	CID (8 keV)	20	10	100	15
8	hybrid (JHI)	CI (H <sub>2</sub> O)	MI	6	3	100	4
		CI (H <sub>2</sub> O)	CID (10 eV)	20	15	100	25

<sup>a</sup> Given relative to the base peak = 100. <sup>b</sup> Chemical ionization (CI) using the indicated reagent gases or electrospray ionization from methanolic solution. <sup>c</sup> For CID, collision energies in the laboratory frame are given.

**TABLE 3: Energetics of the Model Systems [(CH<sub>3</sub>)H<sub>2</sub>NC<sub>6</sub>H<sub>4</sub>CH(R)OCH<sub>3</sub>]<sup>+</sup> Calculated at the B3LYP/6-311G\* Level of Theory: N-Protonated 4-(Methoxymethyl)-N-methylaniline, 8H<sup>+</sup>, with R = H, and N-Protonated 4-((Methoxy)phenylmethyl)-N-methylaniline, 9H<sup>+</sup>, with R = C<sub>6</sub>H<sub>5</sub><sup>a</sup>**

model	R = H	R = C <sub>6</sub> H <sub>5</sub>
[(CH <sub>3</sub> )H <sub>2</sub> NC <sub>6</sub> H <sub>4</sub> CH(R)OCH <sub>3</sub> ] <sup>+</sup>	0	0
[H <sub>2</sub> NC <sub>6</sub> H <sub>4</sub> CH(R)OCH <sub>3</sub> ] <sup>+</sup> + CH <sub>3</sub> <sup>•</sup>	206	198
[(CH <sub>3</sub> )H <sub>2</sub> NC <sub>6</sub> H <sub>4</sub> CH(R)] <sup>+</sup> + CH <sub>3</sub> O <sup>•</sup>	273	242
[H <sub>2</sub> NC <sub>6</sub> H <sub>4</sub> CH(R)] <sup>+</sup> + CH <sub>3</sub> <sup>•</sup> + CH <sub>3</sub> O <sup>•</sup> <sup>b</sup>	362	309
[(CH <sub>3</sub> )HNC <sub>6</sub> H <sub>4</sub> CH(R)] <sup>+</sup> + CH <sub>3</sub> OH	39	-10
[H <sub>2</sub> NC <sub>6</sub> H <sub>4</sub> CH(R)] <sup>+</sup> + CH <sub>3</sub> OCH <sub>3</sub>	47	-6

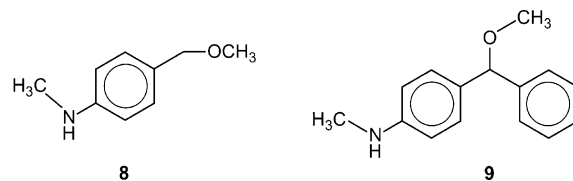
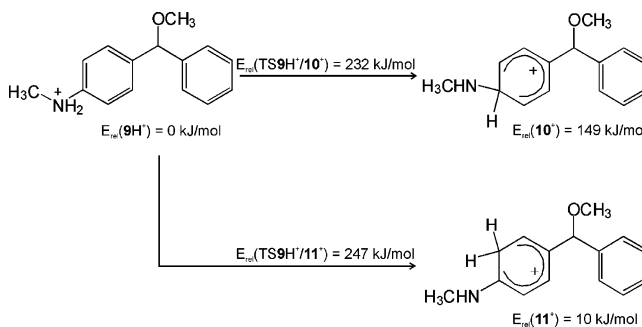
<sup>a</sup> Energies at 0 K given in kJ mol<sup>-1</sup> relative to the protonated anilines 8H<sup>+</sup> and 9H<sup>+</sup>. <sup>b</sup> We note in passing that the computations also show a previously recognized bias of B3LYP with regard to the strength of C–O bonds.<sup>52</sup> Thus, from the fourth and sixth row of the table,  $D(\text{CH}_3\text{O}-\text{CH}_3)$  can be derived as 315 kJ/mol, whereas the experimental value amounts to  $348 \pm 4$  kJ/mol. A similar underestimation occurs for  $D(\text{CH}_3-\text{OH})$ ,<sup>52</sup> and thus the errors are assumed to cancel mostly as far as relative energies are concerned.

conditions. The absence of methanol loss from 3<sup>+</sup> also rules out an alternatively conceivable mobility of the methoxy group.

If both the methyl and the methoxy group in 3<sup>+</sup> do not migrate, the elimination of [C<sub>2</sub>H<sub>6</sub>O] cannot correspond to the formation of intact dimethyl ether but must proceed stepwise.<sup>48–50</sup> While the consecutive expulsion of CH<sub>3</sub><sup>•</sup> and CH<sub>3</sub>O<sup>•</sup> is thermochemically more demanding than formation of CH<sub>3</sub>OCH<sub>3</sub> by  $\Delta E = \text{BDE}(\text{CH}_3\text{O}-\text{CH}_3) = 348$  kJ/mol, the homolytic bond cleavages presumably do not involve energetic barriers in large excess of the thermochemical thresholds; in addition, they are entropically favored. Crucial support for this interpretation comes from the observation of a small amount of methyl loss upon CID of 3<sup>+</sup> (Figure 1). As noted above, the apparent threshold for this fragmentation channel is lower than that for [C<sub>2</sub>H<sub>6</sub>O] loss, thus corroborating the assumed stepwise nature of the latter. The very small abundance of the primary fragment ion ( $m/z = 270$ ) points to a particularly high efficiency of the consecutive CH<sub>3</sub>O<sup>•</sup> elimination. Apparently, the barrier of this reaction is quite low, which is ascribed to the formation of an energetically favored closed-shell species.

The observation of the primary fragment ion might be facilitated if it could be stabilized compared to the product of the consecutive fragmentation. To explore this possibility, two ions structurally related to 3<sup>+</sup>, namely 6H<sup>+</sup> and 7H<sup>+</sup> (Scheme 4), were prepared by ESI of methanolic solutions of 6 and 7, respectively, and subjected to CID.

While 7H<sup>+</sup> shows only slightly enhanced CH<sub>3</sub><sup>•</sup> loss ( $\Delta m = -15$ ) compared to 3<sup>+</sup> (data not shown), this fragmentation channel predominates for 6H<sup>+</sup> at low collision energies (Table 2, entries 1–3). Presumably, the removal of one of the two aromatic rings reduces the stabilization gained by delocalization

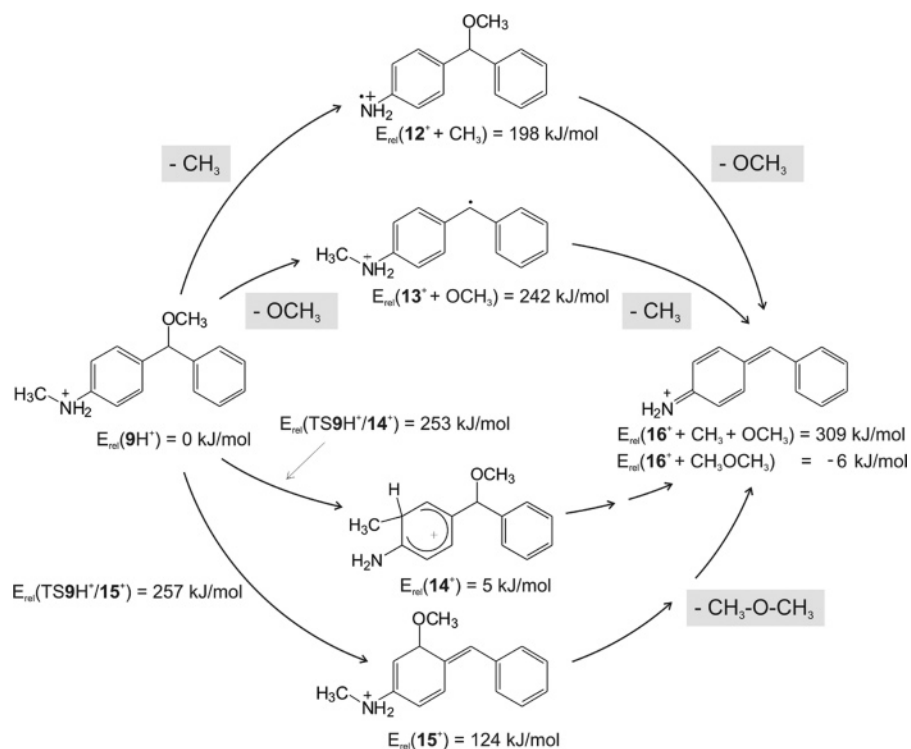
**SCHEME 5****SCHEME 6**

of the positive charge in the final fragmentation product and thus suppresses its formation at lower collision energies. As in the case of 3<sup>+</sup>, the increase of [C<sub>2</sub>H<sub>6</sub>O] loss ( $\Delta m = -46$ ) at higher energies can be easily rationalized by the assumed stepwise nature of this reaction whereas it contradicts the formation of CH<sub>3</sub>OCH<sub>3</sub>. As discussed above for the analogous case of 3<sup>+</sup>, such a process would involve a complex rearrangement, which would be disfavored in the shorter lived collision complexes sampled at higher energies.

The two remaining, minor fragmentation channels comprise loss of methanol CH<sub>3</sub>OH ( $\Delta m = -32$ ; for a rationalization see below) and CH<sub>3</sub>O<sup>•</sup> ( $\Delta m = -31$ ). The latter process provides further evidence for the independent and stepwise expulsion of CH<sub>3</sub><sup>•</sup> and CH<sub>3</sub>O<sup>•</sup> upon CID. Clearly, the loss of CH<sub>3</sub><sup>•</sup> is largely preferred over that of CH<sub>3</sub>O<sup>•</sup>, suggesting that the C–N bonds of the dimethylamino group are more easily cleaved than the C–O bond of the benzylic ether in the first step. Also note that no expulsion of atomic hydrogen is observed. This selective loss of CH<sub>3</sub><sup>•</sup>, rather than H<sup>•</sup>, can be accounted for by the well-known order of bond-dissociation energies, i.e.,  $D(\text{R}_3\text{N}^+-\text{CH}_3) < D(\text{R}_3\text{N}^+-\text{H})$ . In the case of protonated *N,N*-dimethylaniline, for example, the thermochemical data available in the literature<sup>47</sup> imply  $D(\text{C}_6\text{H}_5\text{N}(\text{H})(\text{CH}_3)^+-\text{CH}_3) = 246$  kJ/mol for the C–N bond compared to  $D(\text{C}_6\text{H}_5\text{N}(\text{CH}_3)_2^+-\text{H}) = 316$  kJ/mol for the N–H bond.

In addition, 6H<sup>+</sup> was generated by protonation<sup>35</sup> of neutral 6 with different reagent gases (H<sub>2</sub>O, C<sub>4</sub>H<sub>10</sub>, and NH<sub>3</sub>) in the chemical-ionization source of a sector-field instrument. After mass selection, 6H<sup>+</sup> was then probed by metastable ion (MI)

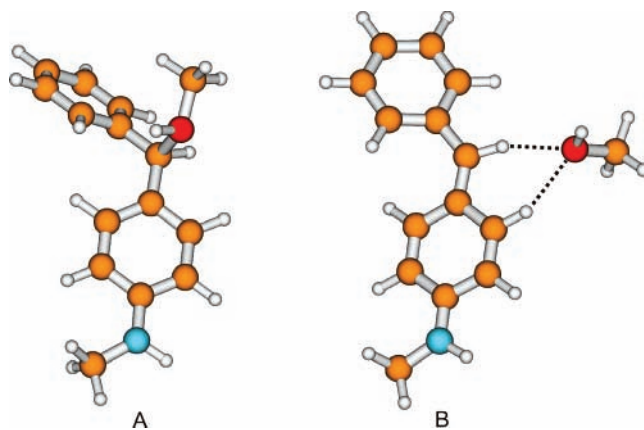
## SCHEME 7



studies as well as CID experiments at keV collision energies. In contrast to  $6\text{H}^+$  produced by ESI,  $6\text{H}^+$  generated by chemical ionization preferentially eliminates  $\text{CH}_3\text{OH}$  ( $\Delta m = -32$ ) upon fragmentation, whereas losses of  $\text{CH}_3^\bullet$  ( $\Delta m = -15$ ),  $\text{CH}_3\text{O}^\bullet$  ( $\Delta m = -31$ ), and  $[\text{C}_2\text{H}_6\text{O}]$  ( $\Delta m = -46$ ) are less pronounced (Table 2, entries 4–7). To test whether this deviating behavior originates from the different ionization method or the different instrumentation, we performed control experiments with a sector-multipole hybrid mass spectrometer. In this instrument,  $6\text{H}^+$  was made via chemical ionization and then probed by low-energy CID in a quadrupole collision cell.<sup>51</sup> Again, predominant elimination of  $\text{CH}_3\text{OH}$  is observed (Table 2, entries 8 and 9), which proves the dependence of the fragmentation pattern on the ionization method rather than on the instrumentation. These findings strongly suggest that different sites of protonation are sampled in the experiments employing different ionization methods: whereas ESI affords the N-protonated ion with a very high selectivity (the small amount of  $\text{CH}_3\text{OH}$  loss observed for  $6\text{H}^+$  produced by ESI indicates the presence of a spurious amount of O-protonated **6**), chemical ionization apparently leads to protonation at all possible sites, i.e., O-protonated **6**, N-protonated **6**, and possibly also ring-protonated **6**. Interestingly, the ratio between O- and N-protonation of **6**, as reflected in the ratio between  $\text{CH}_3\text{OH}$  loss and all remaining fragmentation channels, changes with the reagent gas used for chemical ionization. The higher amount of methyl elimination observed upon application of  $\text{NH}_3$  presumably reflects the high PA of this substrate ( $\text{PA}(\text{NH}_3) = 853.6$ , compared to  $\text{PA}(\text{C}_4\text{H}_{10}) = 643$  and  $\text{PA}(\text{H}_2\text{O}) = 691$  kJ/mol)<sup>47</sup> and the vice versa relatively low gas-phase acidity of its corresponding acid  $\text{NH}_4^+$ . While  $\text{NH}_4^+$  can still efficiently protonate the highly basic dimethylamino group in **6**, protonation of the much less basic methoxy function seems to be disfavored.

With respect to the fragmentation channels indicative of N-protonated **6**, i.e., losses of  $\text{CH}_3^\bullet$ ,  $\text{CH}_3\text{O}^\bullet$ , and  $[\text{C}_2\text{H}_6\text{O}]$ , the results obtained with the sector-field instrument fully support the assumption of stepwise homolytic bond cleavages. Again,

**SCHEME 8 Structure A Optimized at B3LYP/STO-3G and Structure B Optimized at B3LYP/6-311G\* Levels of Theory of Ion  $17^+$** <sup>a</sup>



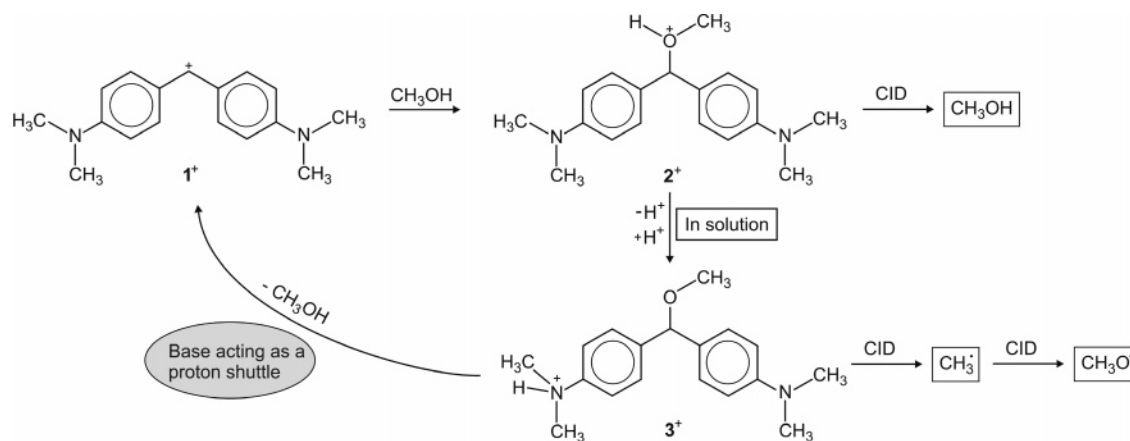
<sup>a</sup> Carbon atoms in orange, oxygen atoms in red, nitrogen atom in blue, and hydrogen atoms in white color.

$\text{CH}_3^\bullet$  loss predominates over  $\text{CH}_3\text{O}^\bullet$  loss, corroborating the lower energy threshold and barrier associated with the former process. Moreover, the loss of  $[\text{C}_2\text{H}_6\text{O}]$  is much more pronounced in CID compared to the metastable ion studies. As explained above, such an energy behavior is incompatible with the occurrence of the complex rearrangement required for the coupling of the N-methyl group with the methoxy function of the ether.

Finally, to substantiate the suggested occurrence of consecutive radical losses by one more experiment, the corresponding cation radicals  $6^{\bullet+}$  and  $7^{\bullet+}$  were investigated as well. As expected, both cation radicals (generated by electron ionization) show abundant and almost exclusive losses of  $\text{CH}_3\text{O}^\bullet$  ( $\Delta m = -31$ ), thereby corroborating the proposed sequence of a stepwise loss of two radicals.

**Computational Studies.** The experiments lead to a qualitative understanding of the chemistry of  $3^+$  and related carbenium ions, yet many important details remain unknown. One key question

## SCHEME 9



in the present context is whether proton migration leading to the dissociation of **3<sup>+</sup>** into **1<sup>+</sup>** +  $\text{CH}_3\text{OH}$  indeed corresponds to an exoergic process or whether the dissociation observed is driven by residual collision energy of the ions in the experiments or their internal energy content. Answers can be provided by contemporary computational chemistry. However, we had to make some compromises in the calculations as far as the level of theory and the complexity of the molecules are concerned. Specifically, the protonated forms of *N*-methyl-4-(methoxymethyl)aniline, **8**, and *N*-methyl-4-(1-methoxy-1-phenylmethyl)aniline, **9**, were investigated (Scheme 5). The calculations employed the hybrid density functional method B3LYP in conjunction with 6-311G\* basis sets.

For compound **8**, the loss of methanol from the energetically preferred N-protonated form is computed to be endothermic by  $39 \text{ kJ mol}^{-1}$ . As expected, loss of dimethyl ether is slightly more energy demanding (Table 3). The introduction of an additional phenyl substituent at the methoxymethyl moiety further stabilizes the carbenium ion resulting after loss of methanol, which is in fact computed to be exothermic for the N-protonated form **9H<sup>+</sup>**. Like for **8H<sup>+</sup>**, the loss of dimethyl ether from **9H<sup>+</sup>** is computed to be slightly more energy demanding than loss of methanol.

As noted above, the chemistry of **3<sup>+</sup>** and related carbenium ions is not just determined by the thermochemical stabilities of the species involved but crucially depends on the barriers pertinent to the different reaction channels. Accordingly, we investigated the potential-energy surface of the model system **9H<sup>+</sup>** in somewhat more detail (Schemes 6 and 7). At first, the migration of the proton from the amino group of **9H<sup>+</sup>** to the adjacent carbon atom of the phenyl ring to form **10<sup>+</sup>** is associated with an energy barrier of  $232 \text{ kJ/mol}$  (Scheme 6). An alternative pathway, where the proton from the amino group migrates directly to the *ortho*-position of the ring, is associated with an even larger energy barrier of  $247 \text{ kJ/mol}$ .

The rather high values of these barriers can explain why the corresponding unimolecular proton migrations are not observed in the experiments. Indeed, the alternatively postulated homolytic bond cleavages are calculated to be less energy-demanding if we assume that they do not involve energy barriers in excess of the thermochemical thresholds. Theory also agrees with experiment in that it predicts a lower threshold for the initial loss of  $\text{CH}_3^\bullet$  compared to that of  $\text{CH}_3\text{O}^\bullet$  (Table 3). In both cases, the subsequent eliminations of a second radical ( $\text{CH}_3\text{O}^\bullet$  or  $\text{CH}_3^\bullet$ , respectively) yielding the closed-shell species involve only low barriers, as was already inferred from experiment. The calculations further predict that the expulsion

of a hydrogen atom from the protonated amino group requires  $260 \text{ kJ/mol}$  and thus confirm the assumption that this reaction channel cannot compete with the elimination of a methyl radical. For the sake of completeness, also migration of the *N*-methyl and the methoxy group are considered. Opposite to hydrogen migration, direct migrations of the *N*-methyl group to the *ortho*-position of the benzene ring is slightly favored compared to that to the *ipso*-position. The rearrangement of the methyl group to the *ortho*-position proceeds with inversion of configuration of the methyl group, as expected from the conservation of orbital symmetry.<sup>53</sup> While the resulting intermediate **14<sup>+</sup>** is almost as stable as **9H<sup>+</sup>**, its formation is associated with an energy barrier of  $253 \text{ kJ/mol}$  (Scheme 7). For comparison, the migration of the methyl group to the *ipso*-position of the ring is subject to an energy barrier of  $264 \text{ kJ/mol}$ . Migration of the methoxy group to the benzene ring is associated with a similar energy demand of  $257 \text{ kJ/mol}$ . Hence, all these rearrangement processes bear significant activation energies and thus cannot compete with the simple loss of a methyl or a methoxy radical. Accordingly, a comprehensive consistent picture of the ion energetics of **9H<sup>+</sup>** evolves from the calculations (Scheme 7).

A similar situation is observed for the smaller model system **8H<sup>+</sup>**, where the initial elimination of a methyl radical requires  $206 \text{ kJ/mol}$  compared to  $273 \text{ kJ/mol}$  for the alternative loss of the methoxy group (Table 3). It is interesting to note that along the fragmentation of the smaller model ion **8H<sup>+</sup>**, somewhat less stabilization is provided for the intermediates as well as for the final product, which leads to larger energy demands for the eliminations of the as compared with the fragmentation larger model compound **9H<sup>+</sup>**. As the experimentally studied ion **3<sup>+</sup>** is even larger, a somewhat larger electronic stabilization of the respective intermediates and of the product **1<sup>+</sup>** can be expected. Hence, the subsequent losses of methyl and methoxy radicals can safely be assumed to be slightly less energy demanding than calculated for the model system **9H<sup>+</sup>**.

In the evaluation of the whole reaction sequence, it is further important to note that the amount of energy required for fragmentation within the time scale of the experiment is significantly larger than the threshold activation energy: Only with this excess amount of energy, unimolecular dissociation proceeds fast enough to yield sufficient fragments and become observable within the experimental time window, a phenomenon referred to as kinetic shift.<sup>54</sup> The internal energy of the fragmenting parent ion will therefore be much larger than the energetic threshold for the first radical loss, which will in turn facilitate the subsequent loss of another radical. With respect to the competition between the subsequent radical losses and

possible rearrangements leading to the formation of intact dimethyl ether, the radical losses are not only the energetically favored processes but also entropically favored because in contrast to the homolytic cleavages of bonds all the rearrangements considered are associated with tight transition structures. Thus, at a given internal energy of the parent ammonium ion, the loss of a methyl or a methoxy radical will always prevail over complex rearrangements. The subsequent loss of the respective second radical is hence also a consequence of the high internal energy content of the parent ion at the beginning of the fragmentation.

Finally, we address the question of the minimum on the potential-energy surface of the system  $1^+ + \text{CH}_3\text{OH}$ . As reaction  $3^+ \rightarrow 1^+ + \text{CH}_3\text{OH}$  is exoergic and cations generally tend to form stable ion/dipole complexes with neutral molecules, the weakly bound methanol adduct of  $1^+$  can be expected to be the most stable species on the potential-energy surface discussed here. Note that such a weakly bound adduct is not observed in the ESI experiments, because it does not survive the conditions in the source, which include multiple collisions with nebulizing and drying gas at a temperature of 80 °C. In contrast, the tautomer  $2^+$ , having a covalent C–O bond, can be safely assumed to be less stable than the N-protonated form  $3^+$  (see above). We have approached this problem by theoretical studies for a model system  $17^+$  (Scheme 8), which is a tautomer of  $9\text{H}^+$  with the proton attached to the oxygen atom (let us reserve the notation  $9\text{H}^+$  for the N-protonated form of **9**). The structure **A** with a covalent C–O bond could be found only with a very small basis set (B3LYP/STO-3G). Optimization of the geometry of  $17^+$  with the double  $\zeta$  and triple  $\zeta$  basis sets always led to minimum **B**, where methanol is bound to the carbenium ion through a hydrogen bond. Complex  $17^+$  (structure **B**) lies 47 kJ/mol lower in energy than its tautomer  $9\text{H}^+$ . Thus, the methanol complex represents the most stable species on the potential-energy surface studied. For comparison, a single-point calculation of the energy at B3LYP/6-311G\* of the ion with structure **A** (corresponding to O-protonation of the neutral compound **9**) suggests that such an isomer would lie 121 kJ/mol above the complex with structure **B** and hence 74 kJ/mol above the N-protonated form  $9\text{H}^+$ . While compared to Michler's hydrol blue, the model system studied bears only one *N*-methyl group and also lacks the dimethylamino group on the second phenyl group, it is reasonable to expect a very similar situation for the system  $1^+/\text{CH}_3\text{OH}$ .

## Conclusions

In the gas phase, the formal methanol adduct of Michler's hydrol blue, a prototypical long-lived, stable carbenium ion, shows a fragmentation via two sequential losses of open-shell fragments and furthermore serves as an example for proton-shuttle catalysis. The complete chemistry of the carbenium ion  $1^+$  can be summarized in terms of Scheme 9. In methanolic solution, a solvent molecule attacks the carbenium ion to yield the O-protonated form of the methoxy compound **5**, that is, cation  $2^+$ . A sequence of deprotonation and reprotonation can then lead to the more stable tautomer  $3^+$ . In the gas phase, however,  $2^+$  and  $3^+$  cannot interconvert and the fragmentation of the N-protonated diarylmethyl ether  $3^+$  is observed with a remarkable selectivity. Upon CID of mass-selected  $3^+$ , sequential losses of first a methyl radical and then the methoxy group take place. Theory suggests that the elimination of  $\text{CH}_3\text{OH}$  is exoergic but hindered by large barriers associated with the proton transfer between the spatially distant nitrogen and oxygen atoms, such that expulsion of  $\text{CH}_3\text{OH}$  does not occur even at

elevated collision energies. This barrier can be circumvented, however, in the presence of an external base which can act as a proton shuttle and transfer a proton from the amino group to the ether oxygen (via intermediate **B**), followed by dissociation into the carbenium ion  $1^+$  and neutral methanol. Hence, a single molecule of an appropriately basic reagent can thus mimic a solvent in its capability to mediate intermolecular proton transfer. The occurrence of such exothermic proton transfers also prevents the use of the otherwise successful kinetic method for the determination of the gas-phase proton affinity of the deprotonated diaryl methyl ether **5**.

**Acknowledgment.** Generous support by the Deutsche Forschungsgemeinschaft, the Fonds der Chemischen Industrie, and the Sanofi-Aventis AG is gratefully acknowledged. J.R. and D.S. thank Dr. Miroslav Polášek for the opportunity to use the sector instrument at the J. Heyrovský Institute for Physical Chemistry (Prague) of the Czech Academy of Sciences. P.G. thanks the Studienstiftung des Deutschen Volkes for a scholarship. Dedicated to Professor David Milstein, Rehovot, in recognition of his fundamental contributions to chemistry on the occasion of his 60th birthday.

**Supporting Information Available:** Complete ref 34. This material is available free of charge via the Internet at <http://pubs.acs.org>.

## References and Notes

- (1) Olah, G. A.; Prakash, G. K. S. *Carbocation Chemistry*; Wiley: Hoboken, NJ, 2004.
- (2) McClelland, R. A. In *Reactive Intermediate Chemistry*; Moss, R. A., Platz, M. S., Jones, M., Jr., Eds.; Wiley: Hoboken, NJ, 2004; p 3.
- (3) Barker, C. C.; Bride, M. H.; Stamp, A. *J. Chem. Soc.* **1959**, 3957.
- (4) Baraldi, I.; Carnevali, A.; Momicchioli, F.; Pontolini, G. *Chem. Phys.* **1992**, *160*, 85.
- (5) (a) Mayr, H.; Bug, T.; Gotta, M. F.; Hering, N.; Irrgang, B.; Janker, B.; Kempf, B.; Loos, R.; Ofial, A. R.; Remmenikov, G.; Schimmel, H. *J. Am. Chem. Soc.* **2001**, *123*, 9500. (b) Ofial, A. R.; Mayr, H. *Angew. Chem., Int. Ed.* **2006**, *45*, 1844.
- (6) Minegishi, S.; Kobayashi, S.; Mayr, H. *J. Am. Chem. Soc.* **2004**, *126*, 5174.
- (7) Kuck, D. In *Encyclopedia of Mass Spectrometry*; Armentrout, P. B., Ed.; Elsevier: Amsterdam, 2003; Vol. 1, p 579.
- (8) O'Hair, R. A. J. In *Encyclopedia of Mass Spectrometry*; Armentrout, P. B., Ed.; Elsevier: Amsterdam, 2003; Vol. 1, p 604.
- (9) Budzikiewicz, H. In *Encyclopedia of Mass Spectrometry*; Nibbering, N. M. M., Ed.; Elsevier: Amsterdam, 2005; Vol. 4, p 470.
- (10) Eberlin, M. N. In *Encyclopedia of Mass Spectrometry*; Nibbering, N. M. M., Ed.; Elsevier: Amsterdam, 2005; Vol. 4, p 483.
- (11) Denekamp, C.; Sanders, Y. *Angew. Chem.* **2006**, *118*, 2147; *Angew. Chem., Int. Ed.* **2006**, *45*, 2093.
- (12) Farneth, W. E.; Brauman, J. I. *J. Am. Chem. Soc.* **1976**, *98*, 7891.
- (13) Laerdahl, J. K.; Uggerud, E. *Int. J. Mass Spectrom.* **2002**, *214*, 277.
- (14) Olmstead, W. N.; Brauman, J. I. *J. Am. Chem. Soc.* **1977**, *99*, 4219.
- (15) Vayner, G.; Houk, K. N.; Jorgensen, W. L.; Brauman, J. I. *J. Am. Chem. Soc.* **2004**, *126*, 9054.
- (16) Lau, Y. K.; Saluja, P. P. S.; Kebarle, P.; Alder, R. W. *J. Am. Chem. Soc.* **1978**, *100*, 7328.
- (17) McMahon, T. B.; Kebarle, P. *J. Am. Chem. Soc.* **1977**, *99*, 2222.
- (18) Fenn, J. B.; Mann, M.; Meng, C. K.; Wong, S. F.; Whitehouse, C. M. *Mass Spectrom. Rev.* **1990**, *9*, 37.
- (19) Smith, R. D.; Loo, J. A.; Loo, R. R. O.; Busman, M.; Udseth, H. R. *Mass Spectrom. Rev.* **1991**, *10*, 359.
- (20) Schröder, D.; Weiske, T.; Schwarz, H. *Int. J. Mass Spectrom.* **2002**, *219*, 729.
- (21) Schröder, D.; Schwarz, H.; Schenk, S.; Anders, E. *Angew. Chem.* **2003**, *115*, 5241; *Angew. Chem., Int. Ed.* **2003**, *42*, 5087.
- (22) Roithová, J.; Hrušák, J.; Schröder, D.; Schwarz, H. *Inorg. Chim. Acta* **2005**, *358*, 4287.
- (23) Schröder, D.; Engeser, M.; Schwarz, H.; Rosenthal, E. C. E.; Döbler, J.; Sauer, J. *Inorg. Chem.* **2006**, *45*, 6235.
- (24) Schröder, D.; Roithová, J. *Angew. Chem.* **2006**, *118*, 5835; *Angew. Chem., Int. Ed.* **2006**, *45*, 5705.



- (25) Schröder, D.; Roithová, J.; Schwarz, H. *Int. J. Mass Spectrom.* **2006**, *254*, 197.
- (26) Schröder, D.; Semialjac, M.; Schwarz, H. *Int. J. Mass Spectrom.* **2004**, *233*, 103.
- (27) Bouchoux, G.; Salpin, J. Y.; Leblanc, D. *Int. J. Mass Spectrom. Ion Processes* **1996**, *153*, 37.
- (28) Schröder, D.; Engeser, M.; Brönstrup, M.; Daniel, C.; Spandl, J.; Hartl, H. *Int. J. Mass Spectrom.* **2003**, *228*, 743.
- (29) Schalley, C. A.; Schröder, D.; Schwarz, H. *Int. J. Mass Spectrom. Ion Processes* **1996**, *153*, 173.
- (30) Yao, C.; Cuadrado-Peinado, M. L.; Poláček, M.; Tureček, F. *Angew. Chem.* **2005**, *117*, 6866; *Angew. Chem., Int. Ed.* **2005**, *44*, 6708.
- (31) Jutz, C. *Chem. Ber.* **1958**, *91*, 850.
- (32) Bertrand, S.; Hoffmann, N.; Humbel, S.; Pete, J. P. *J. Org. Chem.* **2000**, *65*, 8690.
- (33) (a) Vosko, S. H.; Wilk, L.; Nusair, M. *Can. J. Phys.* **1980**, *58*, 1200. (b) Lee, C.; Yang, W.; Parr, R. G. *Phys. Rev. B* **1988**, *37*, 785. (c) Miehlich, B.; Savin, A.; Stoll, H.; Preuss, H. *Chem. Phys. Lett.* **1989**, *157*, 200. (d) Becke, A. D. *J. Chem. Phys.* **1993**, *98*, 5648.
- (34) Frisch, M. J.; et al. *Gaussian 03*, revision C.02; Gaussian, Inc.: Wallingford, CT, 2004.
- (35) Harrison, A. G.; Tu, Y. P. *Int. J. Mass Spectrom.* **2000**, *195*, 33.
- (36) Stewart, J. A.; Shapiro, R. H.; DePuy, C. H.; Bierbaum, V. M. *J. Am. Chem. Soc.* **1977**, *99*, 7650.
- (37) Nobes, R. H.; Radom, L. *Chem. Phys.* **1981**, *60*, 1.
- (38) Ferguson, E. E. *Chem. Phys. Lett.* **1989**, *156*, 319.
- (39) Henchman, M.; Smith, D.; Adams, N. G. *Int. J. Mass Spectrom. Ion Processes* **1991**, *109*, 105.
- (40) Bohme, D. K. *Int. J. Mass Spectrom. Ion Processes* **1992**, *115*, 95.
- (41) Chalk, A. J.; Radom, L. *J. Am. Chem. Soc.* **1997**, *119*, 7573.
- (42) Ausloss, P.; Lias, S. G. *J. Am. Chem. Soc.* **1981**, *103*, 3641.
- (43) Lias, S. G. *J. Phys. Chem.* **1984**, *88*, 4401.
- (44) Zheng, X.; Cooks, R. G.; Augusti, R.; Tao, W. A. In *Encyclopedia of Mass Spectrometry*; Armentrout, P. B., Ed.; Elsevier: Amsterdam, 2003; Vol. 1, p 350.
- (45) Cooks, R. G.; Wong, P. S. H. *Acc. Chem. Res.* **1998**, *31*, 379.
- (46) Complexes (B)H<sup>+</sup>(5) of bases with lower PA could not be generated.
- (47) Thermochemical values taken from the following: *NIST Standard Reference Database Number 69*; NIST: Gaithersburg, MD, 2005; see <http://webbook.nist.gov/chemistry/>.
- (48) Karni, M.; Mandelbaum, A. *Org. Mass Spectrom.* **1980**, *15*, 53.
- (49) Bowen, R. D.; Harrison, A. G. *Org. Mass Spectrom.* **1981**, *16*, 180.
- (50) Ceraulo, L.; Agozzino, P.; Ferrugia, M.; Lamartina, L.; Natoli, M. *C. Org. Mass Spectrom.* **1991**, *26*, 279.
- (51) For a conceptual comparison of low- and high-energy CID, see: Schröder, D. In *Encyclopedia of Mass Spectrometry*; Armentrout, P. B., Ed.; Elsevier: Amsterdam, 2003; Vol. 1, p 460.
- (52) Schröder, D.; Holthausen, M. C.; Schwarz, H. *J. Phys. Chem. B* **2004**, *108*, 14407.
- (53) Carey, F. A.; Sundberg, R. J. *Advanced Organic Chemistry*; Kluwer Academic: New York, 2000.
- (54) Cooks, R. G.; Beynon, J. H.; Caprioli, R. M.; Lester, G. R. *Metastable Ions*; Elsevier: Amsterdam, 1973.